Characterization of Biochar Derived from Pineapple Peel Waste and Its Application for Sorption of Oxytetracycline from Aqueous Solution

Bomin Fu,[a] Chengjun Ge,[a,b,c,*] Lin Yue,[a] Jiwei Luo,[a] Dan Feng,[a] Hui Deng,[d] and Huamei Yu [a,b,*]

Physicochemical characteristics of biochar and its sorption potential for oxytetracycline (OTC) were investigated. Biochars from pineapple peel waste were produced *via* pyrolysis under oxygen-depleted conditions at 350 °C (BL350), 500 °C (BL500), and 650 °C (BL650), as well as the characteristics and polycyclic aromatic hydrocarbons contents of the samples were compared. The sorption kinetics of OTC onto the biochars was completed in three stages, *i.e*., a fast stage, a slow stage, and an equilibrium stage after 24 h. The kinetics data were perfectly fitted by the pseudo-second-order model with high correlation coefficients (R^2 > 0.999). All of the sorption isotherms were nonlinear and well described by the Langmuir model. The Langmuir maximum sorption capacity (q_{max}) increased in the order of BL650 > BL500 > BL350. The thermodynamic parameters revealed that the sorption of OTC onto the biochars was spontaneous and endothermic. Fourier transform infrared spectroscopy (FTIR) of the biochars before and after sorption of OTC confirmed that the H-bonding interaction was the dominant sorption mechanism. The results demonstrated that biochars obtained from inexpensive and renewable materials could be utilized as a highly effective and environmentally friendly adsorbent for removing organic contaminants from wastewater.

Keywords: Biochars; Pineapple peel waste; Characterization; Oxytetracycline; Sorption

*Contact information: a: Department of Environmental Science, Hainan University, Renmin Road, Haikou 570228, China; b: Key Laboratory of Protection and Development Utilization of Tropical Crop Germplasm Resources (Hainan University), Ministry of Education, Renmin Road, Haikou 570228, China; c: Key Laboratory of Environmental Toxicity of Haikou City, Hainan University, Renmin Road, Haikou 570228, China; d: Université de Toulouse; INSA, UPS, INP, 135 Avenue de Rangueil, 31077 Toulouse, France; *Corresponding authors: cjge3007@163.com (C. Ge), yuhuamei3007@163.com (H. Yu).*

INTRODUCTION

Oxytetracycline (OTC) is commonly and widely used in prophylaxis and the treatment of many infectious diseases in humans and animals, and it is recognized for its effective antibacterial properties (Chopra and Roberts 2001; Buchberger 2011). Most OTC is released into different environments through manure spread, sewage irrigation, field runoff, *etc*. (Halling-Sørensen *et al*. 1998). In the past decades, OTC has been frequently detected in liquid manure, soil, groundwater, and surface water, and ranged in concentration from a few ng/L to several μg/L (Lindsey *et al*. 2001). Unfortunately, traditional biological treatment methods are ineffective in degrading OTC because of its persistence and recalcitrance caused by its stable naphthalene ring structure (De Liguoro *et al*. 2003; Liu *et al*. 2015). Therefore, even at low concentrations in the environment, OTC is potentially hazardous and toxic to the health and safety of both humans and aquatic ecosystems (Hirsch *et al*. 1999; Sarmah *et al*. 2006; Lv *et al*. 2012; Rizzo *et al*. 2013). It is

therefore of the utmost importance to develop more efficient treatment technologies for the removal of this contaminant. Several reports indicate that adsorption technology as a physical means is highly effective in eliminating OTC from soil and wastewater (Kong *et al*. 2012; Sun *et al*. 2012).

Biochar, a carbon-rich byproduct, is derived from incomplete combustion and thermal decomposition of biomass under oxygen-depleted conditions (Kookana *et al*. 2011). The application of biochar to soil could help to mitigate global warming by sequestering carbon and reducing emissions of other greenhouse gases (Lehmann 2007). In addition, when added to soils, biochar could increase soil nutrients and crop productivity, and improve the soil's physical and chemical properties, such as water retention and nutrient holding capacity (Glaser *et al*. 2009; Laird *et al*. 2010; Paz-Ferreiro *et al*. 2012). Biochar is an excellent sorbent due to its large specific surface area, abundant microporous structure, high hydrophobicity, and aromaticity (Jonker *et al*. 2004). Biochar could effectively remove various pollutants, such as heavy metals, polycyclic aromatic hydrocarbons (PAHs), steroid hormones, pesticides, and antibiotics (James *et al*. 2005; Sarmah *et al*. 2010; Deng *et al*. 2014; Mohan *et al*. 2014; Feng *et al*. 2015). Thus, biochar can potentially be used as an effective and inexpensive sorbent for adsorbing contaminants from environment.

Pineapple is one of the most common fruits cultivated in tropical and subtropical areas. Its large-scale cultivation and production in food manufacturing industries generates a great deal of waste, such as leaves, stems, peel, *etc*., which is a potential risk in ecosystems and the environment (Foo and Hameed 2012). In this study, pineapple peel waste was chosen as the raw material to produce biochar. This study is valuable in determining uses for agricultural waste. Unfortunately, studies about the sorption behavior of organic contaminants onto biochars derived from pineapple waste are missing. For this reason, the overarching objectives of the present work were to elucidate the differences in three biochars obtained from pineapple peel at different pyrolysis temperatures, to compare and assess the adsorption affinity of OTC onto the different biochars *via* adsorption kinetics, isotherms, and thermodynamics, and to determine the corresponding sorption mechanisms involved *via* Fourier transform infrared spectroscopy (FTIR) before and after the adsorption of OTC. The results obtained might broaden the understanding regarding agricultural waste applications and find an effective way to remove OTC from wastewater.

EXPERIMENTAL

Materials

Oxytetracycline (> 98% purity OTC; 460.43 g/mol molecular weight) was obtained from Dr. Ehrenstorfer company (Berlin, Germany). High performance liquid chromatography (HPLC) grade methanol and acetonitrile was purchased from Sinopharm Chemical Reagent Co. Ltd. (Shanghai, China). Other chemicals were of analytical reagent grade. All aqueous solutions were freshly prepared with ultrapure water acquired from a Spring-S60i+PALL system (Research Scientific Instruments Co. Ltd., Shanghai, China).

Methods

Biochar production

Pineapple peel used for the production of biochar was collected from fruit stores in Haikou City, Hainan Province, China. The waste was air-dried for 3 days and then milled

by a high speed rotary crusher. These samples were pyrolyzed at 200 °C using a muffle furnace under oxygen limited conditions for 2 h. The samples were then heated at a rate of 10 °C/min until the desired temperature was reached (350, 500, and 650 °C) and remained there for 3 h. The prepared biochars were passed through a sieve to achieve an average particle size of 0.15 mm, and they were designated BL350, BL500, or BL650 according to the pyrolysis temperature. These biochars were saved in sealed desiccators until further use.

Characterization of biochar

The yield of biochar was calculated from the dry weight of pineapple peel waste and the mass of the produced biochar after the completion of pyrolysis. The ash contents of the samples were measured from the residual mass after the biochar was heated at 750 °C for 5 h in a muffle furnace.

The pH value of samples was determined by preparing a suspension of biochar and deionized water in a mass ratio of 1:20. The suspension was shaken with a mechanical shaker at 150 rpm for 30 min and equilibrated for 10 min before measuring the pH with a digital pH meter (SG2, Mettler-Toledo. Co. Ltd., Zurich, Switzerland). The cation exchange capacity (CEC) of the samples was measured by the $BaCl_2$-H_2SO_4 forcing exchange method (Zhang *et al*. 2014).

Carbon (C), nitrogen (N), and hydrogen (H) contents in the samples were determined by an elemental analyzer (Vario EL, Elementar, Berlin, Germany). The oxygen (O) content was estimated by mass difference (100 - (C + H + N + ash content)). The atomic ratios of the elements were calculated to estimate the polarity (O/C and (O+N)/C) and aromaticity (H/C) of samples.

The surface morphology and elemental composition of the samples were characterized with a scanning electron microscope (SEM, S-4800, Hitachi, Tokyo, Japan) equipped with an X-ray energy dispersive spectrometry (EDS) detector (3400N, Hitachi, Tokyo, Japan).

The method for extraction and determination of PAHs contents from the samples were referenced by Devi and Saroha (2015).

The pore structure characteristics of the samples were measured by nitrogen adsorption at 77 K with a physical adsorption analyzer (ASAP 2020, Micromeritics Corp., Atlanta, USA). The samples were pretreated by degassing at 300 °C in a vacuum condition for 4 h. The surface area (S_{BET}) was determined by the application of the Brunauer-Emmett-Teller. The total pore volume (V_{total}) was defined as the volume of liquid nitrogen at a high relative pressure of 0.99. The t-plot method was used to estimate the micropore surface area (S_{micro}) and micropore volume (V_{micro}) of the samples. The average pore size (D_{ap}) obtained by the adsorption data using Barrett-Joyner-Halenda (BJH) method.

Sorption experiments

The batch adsorption experiments of OTC onto the biochars were performed. The samples contained 0.1 g of the dried biochar in 10 mL of solution with various initial concentrations (1, 2, 5, 10, 15, and 20 mg/L) of OTC, which were contained in 50 mL centrifuge tubes. The solutions were diluted with a background solution that contained 0.01 M $CaCl_2$ and 200 mg/L of NaN_3 to maintain the ionic strength and inhibit microbial activities. The tubes were shaken at a constant speed of 200 rpm in a mechanical shaker at 15, 25, and 35 °C until equilibrium was reached. After equilibrium was obtained at 24 h (predetermined), the samples were centrifuged at 7000 rpm for 6 min, and the supernatant

liquid was subsequently filtered through a 0.45 μm membrane of polyethersulfone (PES). The residual concentration of OTC in the filtrate was determined immediately by HPLC.

Sorption kinetics was used to investigate the effect of contact time, determine kinetic parameters, and obtain the equilibration time. The samples that contained an initial OTC concentration of 10 mg/L were sampled at the desired time intervals of 0.5, 1, 2, 4, 8, 12, 24, 36, and 48 h at 25 °C. All experiments were conducted in triplicate. In addition, the loss of OTC from the centrifuge tubes was negligible during the sorption without biochar.

The amounts of OTC sorbed onto the biochars were calculated based on the differences between the initial and final solution concentrations according to the following equation,

$$q_e = \frac{(C_0 - C_e)V}{m} \quad (1)$$

where q_e is the amount of OTC adsorbed (mg/g), C_0 is the initial OTC concentration (mg/L), C_e is the equilibrium concentration of OTC (mg/L), V is the volume of solution (L), and m is the mass of adsorbent (g).

Detection of OTC

The concentration of OTC was measured using a Waters 2695 Separations Module HPLC coupled with a 2487 UV detector (Milford, USA). The adsorption wavelength for the detection of OTC was 355 nm. The solutes were separated by a Gemini C18 analytical column (150 × 4.0 mm, 5 μm, Waters) at 35 °C. The mobile phase consisted of acetonitrile and phosphoric acid (0.5‰) (15:85, v/v) at a flow rate of 1 mL/min. The injection volume was fixed to 20 μL, and the retention time for OTC in the HPLC was 4.5 min.

FTIR analysis

FTIR (Nicolet iS10, Thermo Fisher Scientific, Waltham, USA) was used to investigate the changes in the surface functional groups of biochars before and after the adsorption of OTC. The suspensions were removed after the adsorption reached equilibrium (24 h), and then the biochar samples were freeze-dried for FTIR analysis. The dried sample was mixed with KBr in a ratio of 1:100, and the mixture was pressed into a pellet using a tablet machine. The spectra of FTIR were obtained in the wavelength range of 4000 to 400 cm^{-1} at room temperature.

RESULTS AND DISCUSSION

Physicochemical Properties of Biochar

Selected physicochemical characteristics of the samples are listed in Table 1. The biochar yield decreased from 33.94% to 23.74% with increased pyrolysis temperature from 350 °C to 650 °C. The decline in biochar yield mainly corresponded to cellulose-hemicellulose degradation and lignin decomposition with the rise in pyrolysis temperature (Parthasarathy *et al.* 2013). Contrary to the biochar yield, the ash content of the samples noticeably increased, which was mainly due to organic matter loss from the residues and the ash formed from mineral matter after carbonization (Cao and Harris 2010). With respect to CEC, its values increased in the order of BL650 > BL500 > BL350 > pineapple peel, which was similar to the findings reported by Gascó *et al.* (2005). The pH values of

all the biochars were consistently higher than that of the pineapple peel, which was mainly ascribed to the separation of ash content and alkali salts from organic materials at high charring temperatures (Cao and Harris 2010).

When the pyrolysis temperature increased, the C content of the samples increased, whereas the H and O contents decreased. These trends were consistent with the observations of previous studies and were likely because of increased carbonization through dehydration and decarboxylation reactions during high temperature decomposition (Keiluweit *et al*. 2010; Kloss *et al*. 2012). There was no distinct trend for the effect of pyrolysis temperature on N content. In addition, the atomic ratio was calculated to estimate the aromaticity and the polarity of the biochars. The H/C ratio decreased from 0.147 for the raw material to 0.018 for BL650, which indicated an increase in the aromaticity and the formation of highly carbonized biochar. Furthermore, the O/C and (O+N)/C ratios both decreased with a rise in pyrolysis temperature. This was due to a decrease in the O content and increase in the C content after the pyrolysis process, which accounted for the reduction in polarity. These results agreed with the findings reported by Ahmad *et al*. (2012).

The effects of pyrolysis temperature on the surface areas, pore volumes, and pore sizes of the samples are shown in Table 1. With increased charring temperature, the BET surface area (S_{BET}) and micropore surface area (S_{micro}) of the samples increased from 0.352 to 6.643 m^2/g and from 0.304 to 5.708 m^2/g, respectively. It should be noted that the total pore volume (V_{total}) and micropore volume (V_{micro}) of the samples also increased with higher carbonization temperatures, and the maximum values for both were obtained from BL650. The increase in surface area and pore volume with temperature could be attributed to the removal of aliphatic and volatile components during pyrolysis (Keiluweit *et al*. 2010). However, the average pore size (D_{ap}) decreased with increased pyrolysis temperature due to the formation and freeing of additional micropores in the biochars (Novak *et al*. 2009).

Table 1. Characteristics of Pineapple Peel and Its Pyrolysis Biochars at Different Temperatures

Properties	Pineapple peel	BL 350	BL 500	BL 650
Yield (%)	0	33.94	25.74	23.74
Ash (%)	3.97	10.41	12.58	13.23
pH	4.25	9.37	9.57	9.74
CEC (cmol/kg)	49.33	62.17	85.10	116.57
C (%)	41.02	72.95	73.90	74.53
H (%)	6.05	3.36	2.21	1.37
O (%)	48.17	12.05	10.23	9.88
N (%)	0.79	1.23	1.08	0.99
H/C	0.147	0.046	0.030	0.018
O/C	1.174	0.165	0.138	0.133
(O+N)/C	1.194	0.182	0.153	0.146
S_{BET} (m^2/g)	0.352	0.815	2.729	6.643
S_{micro} (m^2/g)	0.304	0.569	2.220	5.708
V_{total} (cm^3/g)	0.0010	0.0015	0.0022	0.0031
V_{micro} (cm^3/g)	0.0001	0.0003	0.0010	0.0026
D_{ap} (nm)	1.376	1.296	1.257	1.106

Table 2. Concentration of PAHs in Pineapple Peel and the Biochars

PAHs (mg/kg)	Pineapple peel	BL 350	BL 500	BL 650	Limits (mg/kg)[a]
Naphthalene (Nap)	0.0249	0.1758	0.0226	0.0210	36
Acenaphthylene (Acpy)	0.0140	0.0232	0.0139	0.0133	–
Acenaphthene (Acp)	0.0164	0.0355	0.0156	0.0160	3700
Fluorene (Flu)	0.0189	0.1061	0.0169	0.0173	2700
Phenanthrene (Phe)	0.0242	0.1998	0.0221	0.0195	–
Anthracene (Ant)	0.0211	0.0732	0.0209	0.0201	22000
Fluoranthene (Fla)	0.0112	0.0427	0.0102	0.0087	2300
Pyrene (Pyr)	0.0317	0.0683	0.0175	0.0146	2300
Benz[a]anthracene (BaA)	0.0062	0.0119	0.0027	0.0025	0.62
Chrysene (CHR)	0.0110	0.0350	0.0098	0.0079	62
Benzo[b]fluoranthene (BbF)	0.0128	0.0108	0.0078	0.0076	0.62
Benzo[k]fluoranthene (BkF)	0.0091	0.0062	0.0051	0.0049	6.2
Benzo[a]pyrene (BaP)	0.0084	0.0070	0.0032	0.0028	0.062
Indeno[1,2,3-cd]pyrene (IND)	0.0250	0.0164	0.0145	0.0142	0.62
Dibenz[a,h]anthracene (DBA)	0.0112	0.0039	0.0021	0.0013	0.062
Benzo[ghi]perylene(Bghip)	0.0133	0.0081	0.0055	0.0052	–
∑16 EPA PAHs	0.2594	0.8239	0.1904	0.1769	20[b]

[a] The standard of residential land quality and human health based preliminary remediation goals for soil (USEPA).

[b] The ∑16 EPA PAHs of maximum allowed thresholds in the biochar (Biochar specification guidelines).

The concentration of 16 PAHs in pineapple peel and biochars are given in Table 2. The amount of BbF, BkF, BaP, IND, DBA, and Bghip in samples decreased with increase in the carbonization temperature due to the volatilization of the amorphous phase, and nuclear condensation of aromatic compounds in non-extractable sheet-like structures in biochars at high temperature (Keiluweit *et al.* 2012). The other PAHs (Nap, Acpy, Acp, Flu, Phe, Ant, Fla, Pyr, BaA, and CHR), as well as total PAHs contents were highest in the BL350, and then decreased with increased pyrolysis temperature, which suggested that the PAHs production occurs in the samples at narrow temperature range. The concentration of PAHs in all the samples were within permissible limits prescribed by the EU (European Union), International Biochar Initiative (IBI) and the United States Environmental Protection Agency (USEPA), which indicated that no environmental implication of usage of biochar derived from pineapple peel waste as an adsorbent (Devi and Saroha 2015; Hilber *et al.* 2012).

SEM-EDS analysis was employed to observe the surface morphologies of samples and to examine the elemental composition of the surface (Fig. 1). Pineapple waste had a distinctly smooth surface and an irregular cylindrical structure at 7000× magnification. The SEM images showed that the surfaces of the biochars became rough with increased pyrolysis temperature, which increased the surface area of the biochars. The EDS analysis suggested that the dominant elements of the localized surface of samples were C, O, and potassium (K). Small amounts of other elements, such as silicon, phosphorus, chlorine, magnesium, and sulfur were also found in the samples.

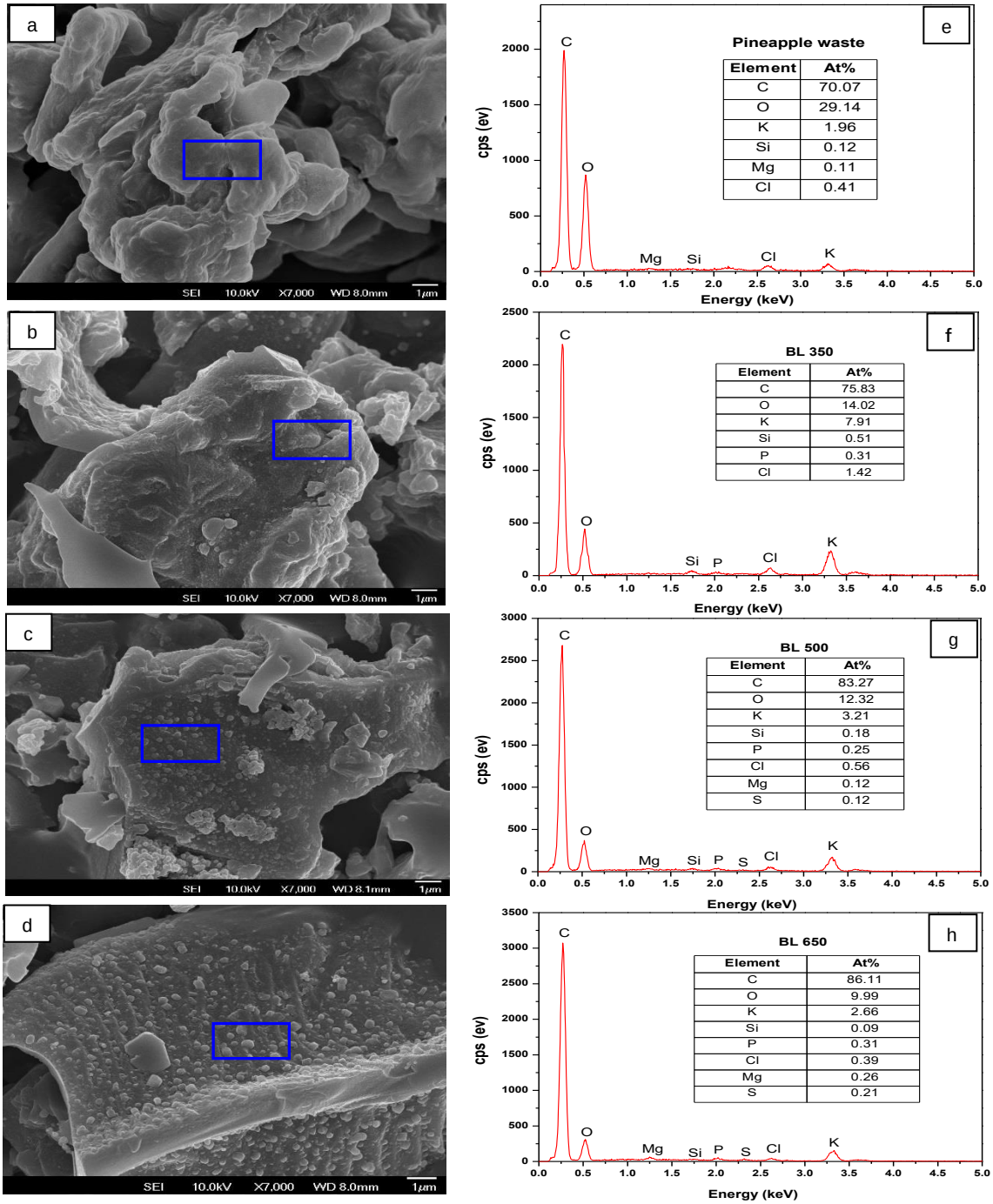

Fig. 1. SEM images (a-d) and corresponding EDS spectra (e-h) for Pineapple waste (a, e), BL350 (b, f), BL500 (c, g), and BL650 (d, h)

Kinetic Studies

The kinetics of OTC sorption onto the three biochars are depicted in Fig. 2. There were three stages in the adsorption process, *i.e.*, the rapid sorption phase, the slow sorption phase, and the equilibrium sorption phase. Approximately 80% of adsorption occurred in the first several hours, and then a slow sorption rate followed until equilibrium was reached after 24 h for all biochars. This was due to the increased driving force from the concentration gradient of the OTC solution and the limited available active adsorption sites

on the biochar surface (Saha *et al.* 2010). Furthermore, the equilibrium sorption capacity of OTC adsorbed onto samples increased with higher pyrolysis temperatures. This was consistent with the larger surface area of the biochar and more adsorption sites produced in the carbonization process.

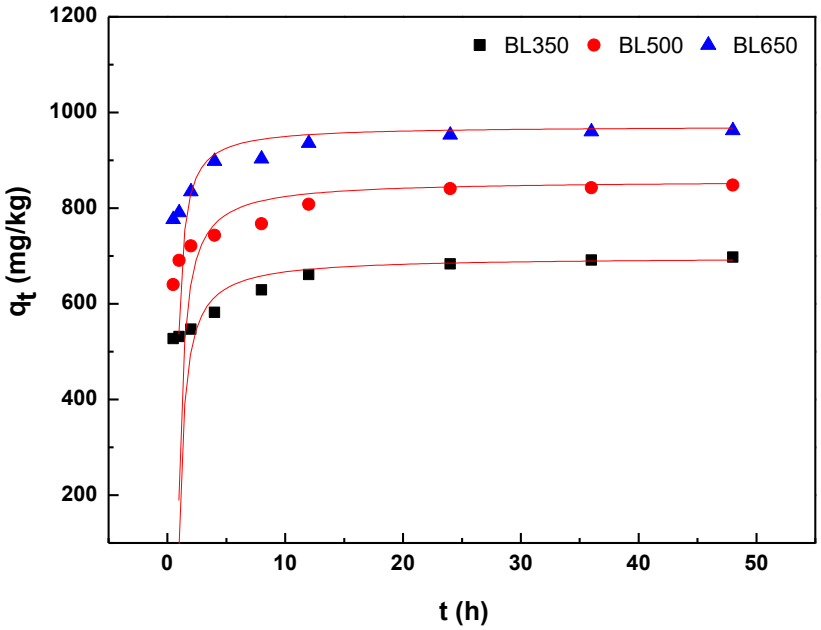

Fig. 2. Adsorption kinetics of OTC onto the three biochars

To quantitatively compare the apparent sorption kinetics between the different biochars, the pseudo-second-order kinetic model (Eq. 2), Elovich model (Eq. 3), and intraparticle diffusion model (Eq. 4) were employed to fit the experimental data by linear regression as follows,

$$\frac{t}{q_t} = \frac{1}{k_2 q_e^2} + \frac{1}{q_e} t \quad (2)$$

$$q_t = a + bt \quad (3)$$

$$q_t = k_p t^{1/2} + C \quad (4)$$

where q_t and q_e are the amounts of OTC adsorbed at time t and at equilibrium (mg/kg), respectively, k_2 is the equilibrium rate constant of pseudo-second-order kinetics adsorption (kg/(mg·h)), a is the rate of initial sorption, b is the sorption activation energy constant, k_p is the intra-particle diffusion rate constant (kg/(mg·$h^{1/2}$)), and C is the thickness of the boundary layer. The values for the adsorption kinetic model parameters and correlation coefficients based on the study data are summarized in Table 3. OTC sorption onto the biochars fit the pseudo-second-order reaction with high correlation coefficients (R^2 > 0.999), which suggested that the experimental data were better fitted by the pseudo second order model than by the Elovich and intraparticle diffusion models. This indicated that the kinetics of the pseudo-second-order model correlated highly with the OTC properties and porous structure of the biochars, and the mechanism of pore diffusion might play a dominant role in the sorption kinetics (Lian *et al*. 2012).

Table 3. Kinetic Parameters for OTC Adsorption onto the Biochars

Biochar	Pseudo-second-order model			Elovich equation			Intraparticle diffusion model		
	q_e (mg/kg)	k_2 (kg/(mg·h))	R^2	a	b	R^2	k_p (kg/(mg·h$^{1/2}$))	C	R^2
BL 350	704.29	0.0025	0.9998	537.10	43.491	0.9611	30.069	519.54	0.8965
BL 500	856.45	0.0029	0.9998	682.86	45.599	0.9820	30.725	667.05	0.8700
BL 650	983.72	0.0033	0.9999	809.10	44.112	0.9565	28.873	796.57	0.7996

Generally, three steps in pseudo-second-order kinetic model are involved, *i.e.*, the migration of the adsorbate molecules from solution to the surface of the adsorbent, the migration of the adsorbate molecules to the internal area of the adsorbent, and the adsorption onto the internal surfaces of the pores of adsorbent (Saha *et al*. 2010; Salima *et al*. 2013). Moreover, the results of the intraparticle diffusion model showed that the plot did not pass through the origin ($C \neq 0$), which further indicated that the adsorption kinetics of OTC onto the biochars was regulated by both surface and intraparticle diffusion (Karagöz *et al.* 2008).

The values of equilibrium adsorption capacity (q_e) from the pseudo-second-order model was much closer to the experimental data and increased with charring temperature, and showed the same trend with the surface area of the biochars.

Isotherm Studies

The adsorption isotherms were used to describe the distribution of both substrates and the solid phases, as well as to understand the essence of adsorbate-adsorbent interactions under an equilibrium state (Almeida *et al.* 2009). Figure 3 shows the equilibrium isotherms for OTC sorption onto the biochars at three different temperatures.

The sorption isotherms of OTC on all the biochars were nonlinear. The biochar was an adsorbent of high heterogeneity. The noncarbonized portion of its structure was characterized by a partition mechanism and displayed linearly, and on the carbonized portion, a pore-filling mechanism with a nonlinear adsorption isotherm occurred (Zheng *et al.* 2010). Therefore, the dominant mechanism for OTC adsorption onto the three biochars was most likely the pore-filling mechanism.

Additionally, the sorption capacity of the biochars improved with the increased temperature from 15 to 35 °C, which suggested that increased sorption temperature facilitated the adsorption of OTC onto the biochars.

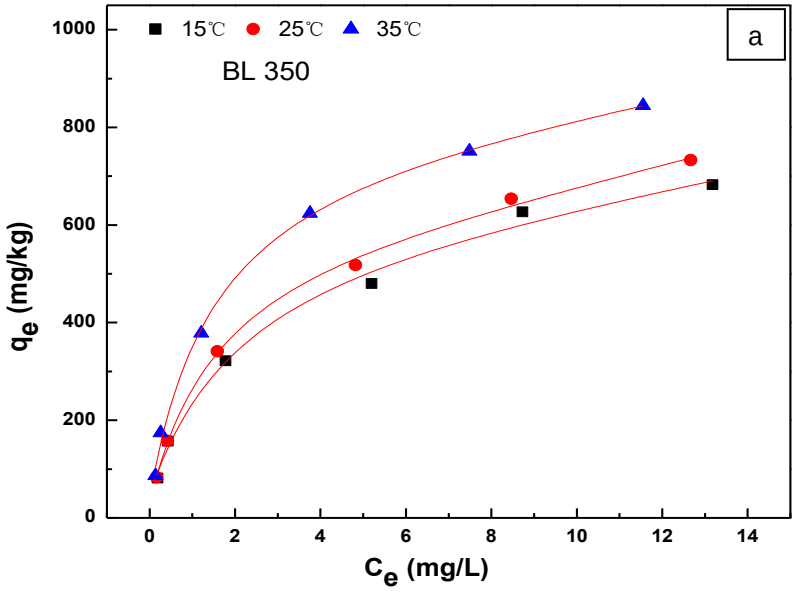

Fig. 3(a). Adsorption isotherms of OTC onto the biochars for BL350 (a), BL500 (b), and BL650 (c)

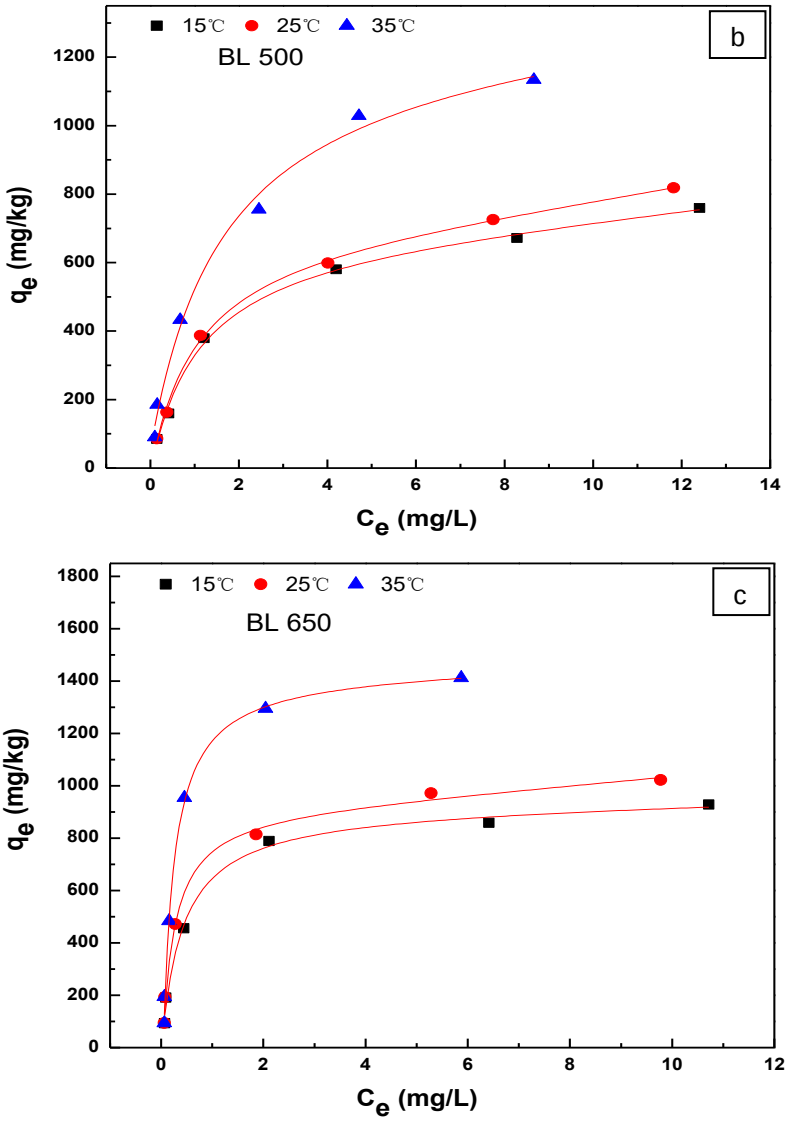

Fig. 3 (b and c). Adsorption isotherms of OTC onto the biochars for BL350 (a), BL500 (b), and BL650 (c)

To further understand the adsorption mechanism, the isotherm equilibrium data were analyzed using the Freundlich (Eq. 5) and Langmuir (Eq. 6) models,

$$\log q_e = \log K_F + \left(\frac{1}{n}\right)\log c_e \quad (5)$$

$$\frac{1}{q_e} = \frac{1}{q_{max}} + \left(\frac{1}{K_L q_{max}}\right)\left(\frac{1}{c_e}\right) \quad (6)$$

where c_e is the equilibrium concentration of OTC (mg/L), q_e is the amount of OTC adsorbed under equilibrium (mg/kg), n is the Freundlich linearity index, q_{max} is the maximum adsorption amount of adsorbent (mg/kg), and K_F and K_L are Freundlich and Langmuir coefficients, respectively.

These two isotherm models were tested to see which fit the experimental data, and the parameters are shown in Table 4. By comparison of the correlation coefficients, it can be seen that the Langmuir model fitted the data slightly better than the Freundlich model, which indicated the presence of monolayer sorption of OTC and homogeneity of the surface active sites on the biochar. The Langmuir maximum sorption capacity (q_{max}) of OTC absorbed on BL350, BL500, and BL650 at 35 °C was about 1.30, 1.51, and 1.66 times greater than that at 15 °C, respectively. The higher temperature seemed to provide the potential activation energy required to change the reactants into the activated complex, and might have had a swelling effect within the pore of sorbent enabling large OTC molecules to penetrate further, thus enhancing the sorption capacity of the biochars (Sun *et al*. 2012).

Table 4. Isotherm Parameters for OTC Sorption onto the Biochars at Different Temperatures

Biochar	Temperature (°C)	Freundlich			Langmuir		
		log K_F	1/n	R^2	K_L	q_{max}(mg/kg)	R^2
BL 350	15	2.3315	0.4877	0.9840	0.8000	698.32	0.9964
	25	2.3619	0.4969	0.9847	0.8888	781.07	0.9933
	35	2.4659	0.4916	0.9665	0.7857	909.14	0.9903
BL 500	15	2.4062	0.4944	0.9594	0.9375	778.41	0.9860
	25	2.4329	0.5086	0.9642	0.8666	897.25	0.9918
	35	2.6323	0.5428	0.9552	0.7000	1176.47	0.9574
BL 650	15	2.6461	0.4112	0.8874	1.5000	945.13	0.9110
	25	2.7023	0.4207	0.8689	1.4000	1072.43	0.8717
	35	2.9165	0.5283	0.8120	1.3380	1568.36	0.8168

Thermodynamic Studies

The adsorption thermodynamics was extremely important to understand the sorption mechanisms of OTC onto the biochar. The thermodynamics parameters such as the Gibbs free energy change ($\Delta G°$), enthalpy change ($\Delta H°$), and entropy change ($\Delta S°$) were determined by using the following equations,

$$\Delta G^{o} = -RT \ln K_F \quad (7)$$

$$\Delta G^{o} = \Delta H^{o} - T\Delta S^{o} \quad (8)$$

where K_F is the Freundlich constant, R is the gas constant (8.314 J/(mol·K)), and T is the absolute temperature (K). The values of $\Delta H°$ and $\Delta S°$ were calculated from the slope and intercept in the linear plot of $\Delta G°$ *versus* T.

The thermodynamic parameters of OTC adsorption are given in Table 5. All the $\Delta G°$ values were negative, which indicated a spontaneous nature and reaction feasibility of OTC sorption onto the biochars at different temperatures. The absolute values of $\Delta G°$ for the biochars increased with the increase in carbonization temperature, which suggested that the higher charring temperature for biochars resulted in a greater degree of spontaneity. Furthermore, $\Delta G°$ became more negative as temperature increased from 15 to 35 °C, which indicated that the driving force for the sorption of OTC increased with higher sorption temperatures. This might have resulted from the larger biochar pore volume and increased OTC adsorption speed onto the internal structure of the biochar at high temperatures (Memon *et al*. 2009). Zhang *et al*. (2014) reported that the value of $\Delta G°$ that ranged from 0 to -20 kJ/mol for physisorption and between -80 to -400 kJ/mol for chemisorption. The

results showed that the values of Δ*G*° ranged from -12.854 to -17.196 kJ/mol, which suggested that the adsorption process might be primarily controlled by physisorption.

In this work, the Δ*H*° values for the sorption process were positive for the three biochars. This indicated that the interaction between OTC and the biochars was an endothermic reaction. Meanwhile, the increase of Δ*H*° with increased carbonization temperature suggested that the sorption process was more endothermic at higher temperatures. The absolute value of Δ*H*° for a sorption process might be used to distinguish between physical (Δ*H*° < 40 kJ/mol) and chemical (Δ*H*° > 40 kJ/mol) adsorption (Feng *et al*. 2013). The values of Δ*H*° ranged from 11.486 to 23.117 kJ/mol, which indicated that the adsorption of OTC was mainly physisorption. Moreover, based on the sorption energy of different forces, the adsorption mechanism of OTC onto the three biochars might have been H-bonding and dipole bond force (von Oepen *et al*. 1991). The entropy change (Δ*S*°) provided a measure for repulsive or binding forces in the system, and was related to the spatial arrangements at the adsorbate-adsorbent interface (Hercigonja *et al*. 2012). In this study, the Δ*S*° values were all positive, which indicated an increase in randomness at the adsorbate-adsorbent interface and high binding affinity of OTC onto the biochars.

Table 5. Thermodynamic Parameters for OTC Sorption onto the Biochars

Biochar	Temperature (°C)	Δ*G*° (kJ/mol)	Δ*H*° (kJ/mol)	Δ*S*° (kJ/(mol·k))
BL 350	15	-12.854	11.486	0.084
	25	-13.474		
	35	-14.540		
BL 500	15	-13.266	19.369	0.113
	25	-13.879		
	35	-15.521		
BL 650	15	-14.589	23.117	0.130
	25	-15.416		
	35	-17.196		

FTIR Analysis

The FTIR spectra (4000 to 400 cm^{-1}) of the biochars before and after OTC adsorption are exhibited in Fig. 4. The broad peaks at about 3400 cm^{-1} were observed due to the stretching vibration of the O-H groups. The band intensities that appeared around 2920 and 2875 cm^{-1} were associated with strong aliphatic C-H stretching vibrations. The C=O stretching vibrations of amides and C=C stretching of the aromatic compounds and benzene ring corresponded to the peaks at approximately 1650, 1570, and 1430 cm^{-1}, respectively. Additionally, the broad bands at 1060 cm^{-1} were due to the C-O asymmetric stretch of alcohols and/or phenolics. Several weak peaks were observed in the region of 850 to 620 cm^{-1} and were determined to be the C-H bending for aromatic out-of-plane deformation. Nevertheless, the disappearance of some distinctive peaks with increased pyrolysis temperature, such as O-H (3400 cm^{-1}), C-H (2920 and 2875 cm^{-1}), and C=O (1650 cm^{-1}) vibrations, suggested there was a breakdown of cellulose and lignin, as well as the removal of hydrogen and oxygen in the carbonization process (Deng *et al*. 2014). It was noted that the peaks at 3400 cm^{-1} (O-H) and 1060 cm^{-1} (C-O) were slightly shifted to 3450 cm^{-1} and 1045 cm^{-1}, respectively, after the sorption of OTC, which indicated the involvement of hydrogen bonding interaction during OTC adsorption (Wahab *et al*. 2010).

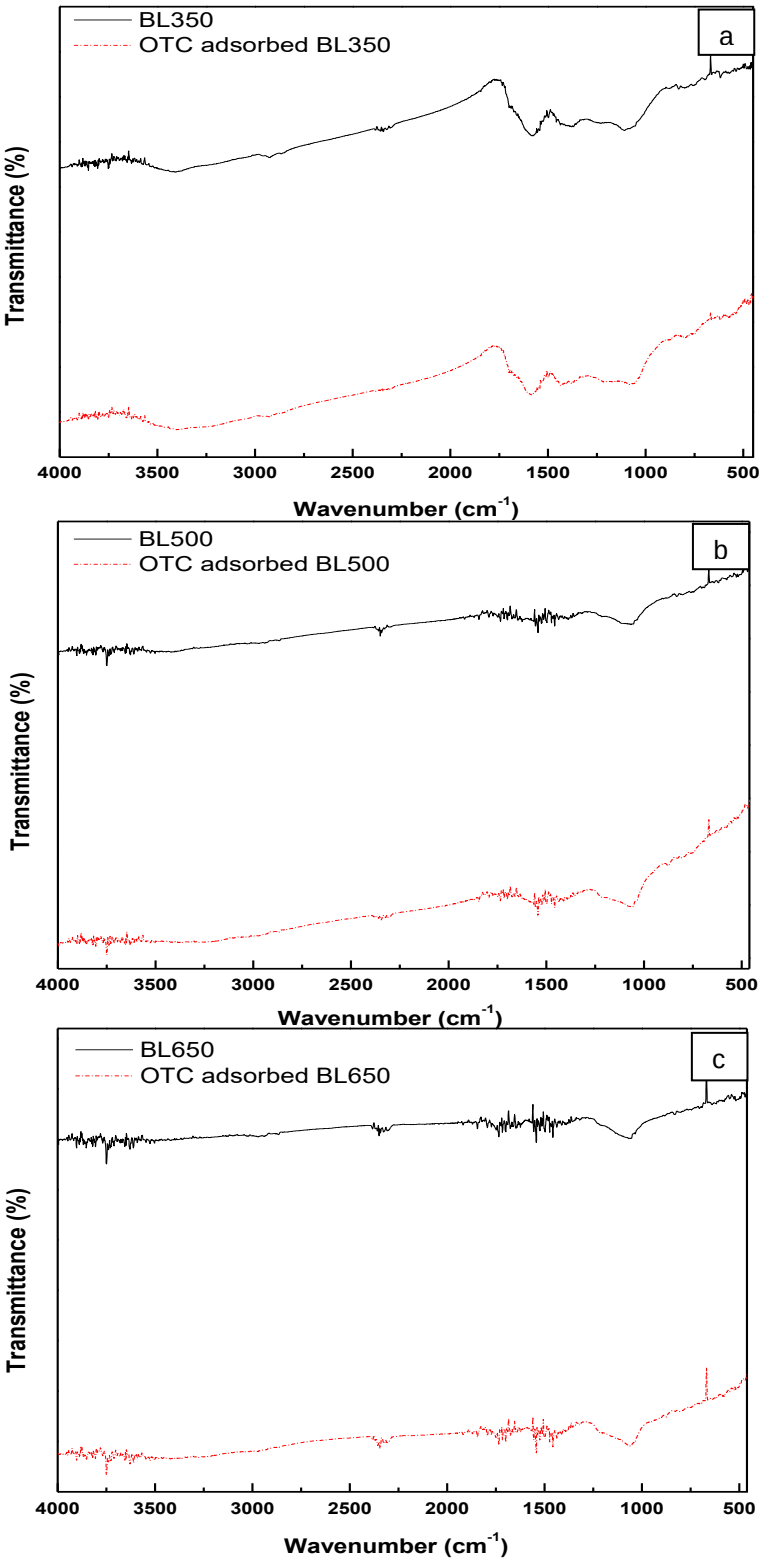

Fig. 4. FTIR spectra for BL350 (a), BL500 (b), and BL650 (c) before and after OTC adsorption

CONCLUSIONS

1. The Ash, pH, CEC, C%, S_{BET}, S_{micro}, V_{total}, and V_{micro} of the samples increased with rise in pyrolysis temperature, whereas the Yield, H%, O%, D_{ap} decreased. The concentration of PAHs in all the biochar were within the prescribed limits.
2. The adsorption capacity of OTC on the biochars was enhanced with the increment of carbonization temperature. The kinetics data were perfectly simulated by the pseudo second order model, and the kinetics process was regulated by both surface and intraparticle diffusion.
3. The Langmuir model could be applied to describe the adsorption isotherm of OTC on the biochars. The sorption isotherms of all the biochars were relatively nonlinear, suggesting pore-filling was the dominant mechanism.
4. Different thermodynamic parameters indicated that the adsorption of OTC on biochars was a spontaneous and an endothermic process, and the sorption interaction of OTC was mainly considered as a physisorption process including hydrogen bonding and dipole bond force.
5. The FTIR analysis confirms that the H-bonding interaction may been a major contribution for the adsorption of OTC onto the biochars.
6. Based on this work, it was concluded that the biochar derived from pineapple peel waste has enormous potential as a renewable, environmentally friendly and effective adsorbent for removing organic contaminants from wastewater. However, the desorption mechanism of biochar and the durable adsorption capacity of the biochar aging should be further investigated.

ACKNOWLEDGMENTS

The authors are grateful for the financial support provided by the National Natural Science Foundation of China (No. 21367011), the National Natural Science Foundation of China (No. 21467008), the Open Fund Program of the Key Laboratory of Protection and Development Utilization of Tropical Crop Germplasm Resources (Hainan University), the Ministry of Education (No. 2013hckled-1), the Natural Science Fund Program of Hainan Province (NO. 413123), and Midwest University Project (MWECSP-RT08, ZXBJH-XK004 and ZXBJH-XK005).

REFERENCES CITED

Ahmad, M., Lee, S. S., Dou, X., Mohan, D., Sung, J. K., Yang, J. E., and Ok, Y. S. (2012). "Effects of pyrolysis temperature on soybean stover and peanut shell-derived biochar properties and TCE adsorption in water," *Bioresource Technol.* 118, 536-544. DOI: 10.1016/j.biortech.2012.05.042

Almeida, C. A. P., Debacher, N. A., Downs, A. J., Cottet, L., and Mello, C. A. D. (2009). "Removal of methylene blue from colored effluents by adsorption on montmorillonite clay," *J. Colloid Interf. Sci.* 332(1), 46-53. DOI: 10.1016/j.jcis.2008.12.012

Buchberger, W. W. (2011). "Current approaches to trace analysis of pharmaceuticals and personal care products in the environment," *J. Chromatogr. A.* 1218(4), 603-618. DOI: 10.1016/j.chroma.2010.10.040

Cao, X., and Harris, W. (2010). "Properties of dairy-manure-derived biochar pertinent to its potential use in remediation," *Bioresource Technol.* 101(14), 5222-5228. DOI: 10.1016/j.biortech.2010.02.052

Chopra, I., and Roberts, M. (2001). "Tetracycline antibiotics: Mode of action, applications, molecular biology, and epidemiology of bacterial resistance," *Microbiol. Mol. Biol. R.* 65(2), 232-260. DOI: 10.1128/MMBR.65.2.232-260.2001

De Liguoro, M., Cibin, V., Capolongo, F., Halling-Sorensen, B., and Montesissa, C. (2003). "Use of oxytetracycline and tylosin in intensive calf farming: Evaluation of transfer to manure and soil," *Chemosphere* 52 (1), 203-212. DOI: 10.1016/S0045-6535(03)00284-4

Deng, H., Yu, H., Chen, M., and Ge, C. (2014). "Sorption of atrazine in tropical soil by biochar prepared from cassava waste," *BioResources* 9(4), 6627-6643. DOI: 10.15376/biores.9.4.6627-6643

Devi, P., and Saroha, A. K. (2015). "Effect of pyrolysis temperature on polycyclic aromatic hydrocarbons toxicity and sorption behaviour of biochars prepared by pyrolysis of paper mill effluent treatment plant sludge," *Bioresource Technol*. 192, 312-320. DOI:10.1016/j.biortech.2015.05.084

Feng, D., Yu, H., Deng, H., Li, F., and Ge, C. (2015). "Adsorption characteristics of norfloxacin by biochar prepared by cassava dreg: Kinetics, isotherms, and thermodynamic analysis," *BioResources* 10(4), 6751-6768. DOI: 10.15376/biores.10.4.6751-6768

Feng, Y., Dionysiou, D. D., Wu, Y., Zhou, H., Xue, L., He, S., and Yang, L. (2013). "Adsorption of dyestuff from aqueous solutions through oxalic acid-modified swede rape straw: Adsorption process and disposal methodology of depleted bioabsorbents," *Bioresource Technol.* 138, 191-197. DOI: 10.1016/j.biortech.2013.03.146

Foo, K. Y., and Hameed, B. H. (2012). "Porous structure and adsorptive properties of pineapple peel based activated carbons prepared *via* microwave assisted KOH and K_2CO_3 activation," *Micropor. Mesopor. Mat.* 148(1), 191-195. DOI: 10.1016/j.micromeso.2011.08.005

Gascó, G., Blanco, C. G., Guerrero, F., and Méndez Lázaro, A. M. (2005). "The influence of organic matter on sewage sludge pyrolysis," *J. Anal. Appl. Pyro.* 74(1-2), 413-420. DOI: 10.1016/j.jaap.2004.08.007

Glaser, B., Parr, M., Braun, C., and Kopolo, G. (2009). "Biochar is carbon negative," *Nature Geoscience* 2(1), 2. DOI: 10.1038/ngeo395

Halling-Sørensen, B., Nors Nielsen, S., Lanzky, P. F., Ingerslev, F., Holten Lützhøft, H. C., and Jørgensen, S. E. (1998). "Occurrence, fate and effects of pharmaceutical substances in the environment - A review," *Chemosphere* 36 (2), 357-393. DOI: 10.1016/S0045-6535(97)00354-8

Hercigonja, R., Rac, V., Rakic, V., and Auroux, A. (2012). "Enthalpy-entropy compensation for n-hexane adsorption on HZSM-5 containing transition metal ions," *J. Chem. Thermodyn*. 48, 112-117. DOI: 10.1016/j.jct.2011.12.016

Hilber, I., Blum, F., Leifeld, J., Schmidt, H. P., and Bucheli, T. D. (2012). "Quantitative determination of pahs in biochar: A prerequisite to ensure its quality and safe application," *J. Agric. Food Chem.* 60(12), 3042-3050. DOI: 10.1021/jf205278v

Hirsch, R., Ternes, T., Haberer, K., and Kratz, K. L. (1999). "Occurrence of antibiotics in the aquatic environment," *Sci. Total Environ*. 225(1-2), 109-118. DOI: 10.1016/S0048-9697(98)00337-4

James, G., Sabatini, D. A., Chiou, C. T., Rutherford, D., Scott, A. C., and Karapanagioti, H. K. (2005). "Evaluating phenanthrene sorption on various wood chars," *Water Res*. 39(4), 549-558. DOI: 10.1016/j.watres.2004.10.015

Jonker, M. T. O., Hoenderboom, A. M., and Koelmans, A. A. (2004). "Effects of sedimentary sootlike materials on bioaccumulation and sorption of polychlorinated biphenyls," *Environ. Toxicol. Chem*. 23(11), 2563-2570. DOI: 10.1897/03-351

Karagöz, S., Tay, T., Ucar, S., and Erdem, M. (2008). "Activated carbons from waste biomass by sulfuric acid activation and their use on methylene blue adsorption," *Bioresource Technol*. 99(14), 6214-6222. DOI: 10.1016/j.biortech.2007.12.019

Keiluweit, M., Kleber, M., Sparrow, M. A., Simoneit, B. R. T., and Prahl, F. G. (2012). "Solvent-extractable polycyclic aromatic hydrocarbons in biochar: influence of pyrolysis temperature and feedstock," *Environ. Sci. Technol*. 46(17), 9333-9341. DOI: 10.1021/es302125k

Keiluweit, M., Nico, P. S., Johnson, M. G., and Kleber, M. (2010). "Dynamic molecular structure of plant biomass-derived black carbon (biochar)," *Environ. Sci. Technol*. 44(4), 1247-1253. DOI: 10.1021/es9031419

Kloss, S., Zehetner, F., Dellantonio, A., Hamid, R., Ottner, F., Liedtke, V., Schwanninger, M., Gerzabek, M. H., and Soja, G. (2012). "Characterization of slow pyrolysis biochars: Effects of feedstocks and pyrolysis temperature on biochar properties," *J. Environ. Qual*. 41(4), 990-1000. DOI: 10.2134/jeq2011.0070.

Kong, W., Li, C., Dolhi, J. M., Li, S., He, J., and Qiao, M. (2012). "Characteristics of oxytetracycline sorption and potential bioavailability in soils with various physical-chemical properties," *Chemosphere* 87(5), 542-548. DOI: 10.1016/j.chemosphere.2011.12.062

Kookana, R. S., Sarmah, A. K., Van Zwieten, L., Krull, E., and Singh, B. (2011). "Biochar application to soil: Agronomic and environmental benefits and unintended consequences," *Adv. Agron.* 112, 103-143. DOI: 10.1016/B978-0-12-385538-1.00003-2

Laird, D., Fleming, P., Wang, B., Horton, R., and Karlen, D. (2010). "Biochar impact on nutrient leaching from a midwestern agricultural soil," *Geoderma* 158(3-4), 436-442. DOI: 10.1016/j.geoderma.2010.05.012

Lehmann, J. (2007). "A handful of carbon," *Nature* 447(7141), 143-144. DOI: 10.1038/447143a

Lian, F., Chang, C., Du, Yang., Zhu, L., Xing, B., and Liu, C. (2012). "Adsorptive removal of hydrophobic organic compounds by carbonaceous adsorbents: A comparative study of waste-polymer-based, coal-based activated carbon, and carbon nanotubes," *J. Environ. Sci.* 24(9), 1549-1558. DOI: 10.1016/S1001-0742(11)60984-4

Lindsey, M. E., Meyer, M. T., and Thurman, E. M. (2001). "Analysis of trace levels of sulfonamide and tetracycline antimicrobials in groundwater and surface water using solid-phase extraction and liquid chromatography/mass spectrometry," *Anal. Chem*. 73(19), 4640-4646. DOI: 10.1021/ac010514w

Liu, Y., He, X., Duan, X., Fu, Y., and Dionysiou, D. D. (2015). "Photochemical degradation of oxytetracycline: Influence of pH and role of carbonate radical," *Chem. Eng. J.* 276, 113-121. DOI: 10.1016/j.cej.2015.04.048

Lv, Y. K., Wang, L. M., Yang, L., Zhao, C. X., and Sun, H. W. (2012). "Synthesis and application of molecularly imprinted poly(methacrylic acid)-silica hybrid composite material for selective solid-phase extraction and high-performance liquid chromatography determination of oxytetracycline residues in milk," *J. Chromatogr. A.* 1227(5), 48-53. DOI: 10.1016/j.chroma.2011.12.108

Memon, G. Z., Bhanger, M. I., Memon, J. R., and Akhtar, M. (2009). "Adsorption of methyl parathion from aqueous solutions using mango kernels: Equilibrium, kinetic and thermodynamic studies," *Bioremediation Journal* 13(2), 102-106. DOI: 10.1080/10889860902902081

Mohan, D., Sarswat, A., Ok, Y. S., and Pittman, C. U. (2014). "Organic and inorganic contaminants removal from water with biochar, a renewable, low cost and sustainable adsorbent - A critical review," *Bioresource Technol*. 160, 191-202. DOI: 10.1016/j.biortech.2014.01.120

Novak, J. M., Lima, I., Xing, B., Gaskin, J. W., Steiner, C., Das, K. C., Ahmedna, M., Rehrah, D., Watts, D. W., Busscher, W. J., and Schomberg, H. (2009). "Characterization of designer biochar produced at different temperatures and their effects on a loamy sand," *Annals of Environmental Science* 3, 195-206.

Parthasarathy, P., Narayanan, K. S., and Arockiam, L. (2013). "Study on kinetic parameters of different biomass samples using thermo-gravimetric analysis," *Biomass Bioenerg.* 58, 58-66. DOI: 10.1016/j.biombioe.2013.08.004

Paz-Ferreiro, J., Gascó, G., Gutiérrez, B., and Méndez, A. (2012). "Soil biochemical activities and the geometric mean of enzyme activities after application of sewage sludge and sewage sludge biochar to soil," *Biol. Fert. Soils* 48(5), 511-517. DOI: 10.1007/s00374-011-0644-3

Rizzo, L., Manaia, C., Merlin, C., Schwartz, T., Dagot, C., Ploy, M. C., Michael, I., and Fatta-Kassinos, D. (2013). "Urban wastewater treatment plants as hotspots for antibiotic resistant bacteria and genes spread into the environment: A review," *Sci. Total Environ*. 447, 345-360. DOI: 10.1016/j.scitotenv.2013.01.032

Saha, P., Chowdhury, S., Gupta, S., and Kumar, I. (2010). "Insight into adsorption equilibrium, kinetics and thermodynamics of malachite green onto clayey soil of Indian origin," *Chem. Eng. J.* 165(3), 874-882. DOI: 10.1016/j.cej.2010.10.048

Salima, A., Benaouda, B., Noureddine, B., and Duclaux, L. (2013). "Application of *Ulva lactuca* and *Systoceira stricta* algae-based activated carbons to hazardous cationic dyes removal from industrial effluents," *Water Res.* 47(10), 3375-3388. DOI: 10.1016/j.watres.2013.03.038

Sarmah, A. K., Meyer, M. T., and Boxall, A. B. A. (2006). "A global perspective on the use, sales, exposure pathways, occurrence, fate and effects of veterinary antibiotics (VAs) in the environment," *Chemosphere* 65(5), 725-759. DOI: 10.1016/j.chemosphere.2006.03.026

Sarmah, A. K., Srinivasan, P., Smernik, R. J., Manley-Harris, M., Antal, M. J., Downie, A., and Van Zwieten, L. (2010). "Retention capacity of biochar-amended New Zealand dairy farm soil for an estrogenic steroid hormone and its primary metabolite," *Aust. J. Soil Res*. 48(6), 648-658. DOI: 10.1071/SR10013

Sun, Y., Yue, Q., Gao, B., Li, Q., Huang, L., Yao, F., and Xu, X. (2012). "Preparation of activated carbon derived from cotton linter fibers by fused NaOH activation and its

application for oxytetracycline (OTC) adsorption," *J. Colloid Interf. Sci*. 368(1), 521-527. DOI: 10.1016/j.jcis.2011.10.067

von Oepen, B., Kördel, W., and Klein, W. (1991). "Sorption of nonpolar and polar compounds to soils: Processes, measurements and experience with the applicability of the modified OECD-Guideline 106," *Chemosphere* 22(3-4), 285-304. DOI: 10.1016/0045-6535(91)90318-8

Wahab, M. A., Jellali, S., and Jedidi, N. (2010). "Ammonium biosorption onto sawdust: FTIR analysis, kinetics and adsorption isotherms modeling," *Bioresource Technol.* 101(14), 5070-5075. DOI: 10.1016/j.biortech.2010.01.121

Zhang, J., Wu, C., Jia, A., and Hu, B. (2014). "Kinetics, equilibrium, and thermodynamics of the sorption of *p*-nitrophenol on two variable charge soils of Southern China," *Appl. Surf. Sci.* 298, 95-101. DOI: 10.1016/j.apsusc.2014.01.130

Zheng, W., Guo, M., Chow, T., Bennett, D. N., and Rajagopalan, N. (2010). "Sorption properties of greenwaste biochar for two triazine pesticides," *J. Hazard. Mater.* 181(1-3), 121-126. DOI: 10.1016/j.jhazmat.2010.04.103

Article submitted: June 18, 2016; Peer review completed: August 20, 2016; Revised version received and accepted: August 29, 2016; Published: September 7, 2016.
DOI: 10.15376/biores.11.4.9017-9035